Exploring Enhancement Mechanisms in Surface-Enhanced Raman Spectroscopy Using Plasmonic Nanostructures

1Kotte Hima Sekhar, 2Yanala Srinivasa Reddy
1Research Scholar, Department of Physics, Bharathiya Engineering Science and Technology Innovation University, Gorantla, Sri Sathya Sai District
Email: himasekharkotte@gmail.com
2Assistant Professor, Department of Physics, Chaitanya Bharathi Institute of Technology, Hyderabad, Telangana
Email: ysreddy_physics@cbit.ac.in

Abstract

Surface Enhanced Raman Spectroscopy (SERS) has emerged as a powerful analytical technique capable of single-molecule detection and chemical characterization with unprecedented sensitivity. This research investigates the fundamental enhancement mechanisms underlying SERS, focusing specifically on the role of plasmonic nanostructures in generating signal amplification. Through comprehensive experimental analysis and theoretical modeling, this study examines how various nanostructure geometries, compositions, and arrangements affect electromagnetic field enhancement and chemical enhancement pathways. Gold and silver nanoparticles of different morphologies were synthesized, characterized, and evaluated for their SERS performance using model analytes. The results demonstrate that the electromagnetic enhancement mechanism contributes approximately 10^6-10^8 to the overall enhancement, while chemical enhancement provides an additional 10^2-10^3 factor. Hot spots generated at the junctions between nanoparticles were found to produce the most significant enhancement, with field intensity increasing exponentially as interparticle distance decreased below 2 nm. This research also proposes a novel hierarchical nanostructure design that optimizes both enhancement mechanisms simultaneously, achieving attomolar detection limits. These findings contribute to the fundamental understanding of SERS enhancement mechanisms and provide practical guidelines for designing more effective SERS substrates for advanced sensing applications.

Keywords-Surface Enhanced Raman Spectroscopy, Plasmonic Nanostructures, Electromagnetic Enhancement, Chemical Enhancement, Hot Spots, Gold Nanoparticles, Silver Nanoparticles, Localized Surface Plasmon Resonance, Near-field Enhancement, Single-molecule Detection

1. Introduction

Raman spectroscopy, discovered by C.V. Raman in 1928, provides valuable information about molecular vibrations and structure through inelastic scattering of light [1]. However, conventional Raman spectroscopy suffers from inherently weak signals, with typically only one in 10^6-10^8 scattered photons undergoing Raman scattering. This fundamental limitation severely restricted the technique's practical applications until the serendipitous discovery of Surface Enhanced Raman Spectroscopy (SERS) by Fleischmann, Hendra, and McQuillan in 1974 when they observed unexpectedly intense Raman signals from pyridine adsorbed on roughened silver electrodes [2].

The subsequent decades have witnessed remarkable progress in understanding and applying SERS, which can enhance Raman signals by factors of 10^6-10^11, enabling even single-molecule detection under optimal conditions. This extraordinary enhancement has positioned SERS as a powerful analytical technique with applications spanning environmental monitoring, food safety, biomedical diagnostics, and fundamental chemical research [3].

The enhancement mechanisms underlying SERS are complex and remain the subject of intensive research. Two primary mechanisms have been identified: electromagnetic enhancement arising from the excitation of localized surface plasmon resonances (LSPRs) in metallic nanostructures, and chemical enhancement resulting from electronic coupling between the adsorbate and substrate [4]. While electromagnetic enhancement is generally accepted as the dominant contribution, providing enhancement factors of 10^4-10^8, the chemical mechanism can contribute an additional 10^2-10^3 factor under appropriate conditions.

Plasmonic nanostructures play a pivotal role in SERS, serving as amplification platforms through their ability to concentrate electromagnetic fields into nanoscale volumes. The size, shape, composition, and arrangement of these nanostructures critically influence their plasmonic properties and, consequently, their SERS performance [5]. Nanostructure design has thus become a central focus in advancing SERS technology, with researchers continuously developing novel architectures to maximize enhancement while maintaining reproducibility and stability.

This research paper investigates the fundamental enhancement mechanisms in SERS through a systematic study of plasmonic nanostructures. By correlating nanostructure properties with SERS performance and developing theoretical models to explain observed phenomena, this work aims to deepen our understanding of the enhancement processes and provide guidelines for designing optimized SERS substrates for various applications.

2. Objectives

The primary objectives of this research are:

1. To elucidate the relative contributions of electromagnetic and chemical enhancement mechanisms in SERS through systematic experimental studies and theoretical modeling.
2. To investigate how nanostructure parameters—including size, shape, composition, and spatial arrangement—influence SERS enhancement factors and spectral characteristics.
3. To identify and characterize "hot spots" in plasmonic nanostructures and quantify their contribution to the overall SERS signal.
4. To develop and validate computational models that accurately predict SERS enhancement based on nanostructure properties.
5. To design and synthesize novel plasmonic nanostructures that optimize both electromagnetic and chemical enhancement mechanisms.
6. To establish practical guidelines for tailoring plasmonic nanostructures for specific SERS applications.

3. Scope of Study

This research encompasses several interconnected areas to provide a comprehensive understanding of SERS enhancement mechanisms:

The study focuses primarily on gold and silver nanostructures, which represent the most widely used and effective SERS substrates due to their favorable plasmonic properties in the visible to near-infrared spectral range. Various nanostructure morphologies are examined, including spheres, rods, cubes, triangular prisms, and hierarchical assemblies, to establish structure-property relationships.

Both experimental characterization and theoretical modeling approaches are employed to develop a complete picture of enhancement mechanisms. Experimental techniques include electron microscopy, spectroscopy, and single-particle studies, while theoretical approaches encompass discrete dipole approximation, finite-difference time-domain simulations, and density functional theory calculations.

The investigation extends to both isolated nanostructures and coupled systems, with particular attention to the enhancement phenomena occurring at junctions between adjacent nanoparticles—so-called "hot spots" that often dominate the overall SERS response.

Model analyte molecules with well-characterized Raman signatures are utilized to assess SERS performance, enabling direct comparisons between different substrates and conditions while minimizing variables associated with the analyte itself.

Environmental factors affecting SERS enhancement, including solvent effects, pH, ionic strength, and temperature, are systematically evaluated to establish their influence on enhancement mechanisms.

Practical considerations such as substrate reproducibility, stability, reusability, and cost-effectiveness are also addressed to ensure that findings can translate to real-world applications.

4. Limitations of the Study

Despite the comprehensive approach employed in this research, several limitations should be acknowledged:

The study primarily focuses on gold and silver nanostructures, with more limited exploration of alternative plasmonic materials such as aluminum, copper, or platinum. These alternative materials may offer advantages for specific applications or wavelength ranges but are not comprehensively evaluated here.

While efforts are made to correlate single-particle properties with ensemble measurements, inherent heterogeneity in nanoparticle samples introduces some uncertainty in structure-property relationships. Perfect monodispersity remains challenging to achieve despite advanced synthesis techniques.

Theoretical models necessarily incorporate approximations and idealizations that may not fully capture the complexity of real experimental systems, particularly regarding surface roughness, ligand effects, and charge transfer processes at the molecule-metal interface.

Quantitative determination of absolute enhancement factors remains challenging due to variations in experimental conditions and measurement methodologies across the field. This study adopts standardized protocols to enable relative comparisons but acknowledges the difficulty in establishing universally comparable absolute enhancement values.

Long-term stability studies are limited by the timeframe of the research, potentially overlooking degradation mechanisms that emerge over extended periods under real-world conditions.

The investigation primarily employs model analytes rather than complex real-world samples, which may introduce additional complexities not fully addressed in the current study.

Computational limitations restrict the size and complexity of systems that can be modeled at high levels of theory, necessitating some compromise between accuracy and computational feasibility.

5. Literature Review

The discovery of SERS is generally attributed to Fleischmann et al., who in 1974 observed unexpectedly intense Raman signals from pyridine adsorbed on electrochemically roughened silver electrodes [2]. Initially, this enhancement was attributed simply to increased surface area, but subsequent work by Jeanmaire and Van Duyne [6] and independently by Albrecht and Creighton [7] in 1977 demonstrated that the enhancement was far too large to be explained by surface area effects alone. These researchers proposed that electromagnetic mechanisms related to the excitation of surface plasmons must be responsible for the majority of the enhancement.

Moskovits made significant contributions to the theoretical understanding of the electromagnetic enhancement mechanism in the 1980s, developing models that related SERS enhancement to the amplification of local electromagnetic fields near metallic surfaces [8]. His work established that SERS enhancement scales approximately with the fourth power of the local electric field, explaining the extreme sensitivity of the technique.

The chemical enhancement mechanism was first proposed by Otto et al. [9], who observed enhancement even when electromagnetic factors were controlled for. This mechanism involves electronic coupling between the molecule and substrate, potentially including charge transfer, molecular resonance effects, and changes in polarizability upon adsorption.

Nie and Emory [10] and Kneipp et al. [11] independently reported single-molecule SERS detection in 1997, demonstrating enhancement factors of approximately 10^14, which far exceeded theoretical predictions based solely on electromagnetic enhancement. These groundbreaking studies highlighted the existence of "hot spots"—regions of extraordinarily high enhancement typically located at junctions between nanoparticles or at sharp features.

Since these seminal works, research has progressed along several fronts. Advancement in nanofabrication techniques has enabled the production of increasingly well-defined SERS substrates. Top-down approaches include electron-beam lithography and nanoimprint lithography, while bottom-up approaches encompass controlled colloidal synthesis and self-assembly [12]. These methods have facilitated the systematic study of how nanostructure parameters influence SERS performance.

Theoretical and computational methods have evolved significantly, with finite-difference time-

domain (FDTD) simulations becoming a standard tool for predicting electromagnetic field distributions around plasmonic nanostructures [13]. These simulations have revealed the critical importance of interparticle spacing, sharp features, and resonance conditions in generating strong enhancement.

Recent research has increasingly focused on practical applications of SERS. In biomedical diagnostics, SERS-based assays have been developed for detecting disease biomarkers at clinically relevant concentrations [14]. Environmental monitoring applications have leveraged SERS for detecting trace contaminants in water and air [15]. Food safety applications include the detection of pesticides, antibiotics, and foodborne pathogens [16].

Despite these advances, several areas remain actively researched. The precise contribution of chemical enhancement continues to be debated, with estimates ranging from negligible to factors of 10^2-10^3 depending on the system [17]. The development of reproducible substrates with consistent enhancement factors remains challenging, particularly for quantitative applications [18]. The extension of SERS to non-traditional plasmonic materials is also an emerging area, with materials such as aluminum, graphene, and semiconductors showing promise for specific applications [19].

This research builds upon this rich literature foundation, addressing current knowledge gaps regarding the interplay between electromagnetic and chemical enhancement mechanisms, the quantitative relationship between nanostructure properties and enhancement factors, and the development of reproducible substrates with optimized performance characteristics.

6. Conceptual Background

Surface Enhanced Raman Spectroscopy operates through two primary enhancement mechanisms: electromagnetic enhancement and chemical enhancement. Understanding these mechanisms requires a conceptual foundation in several interconnected areas.

6.1 Raman Scattering Fundamentals

Raman scattering is an inelastic light scattering process where photons interact with molecular vibrations, resulting in scattered photons with shifted frequencies. The Raman scattering intensity (IR) for a molecule is proportional to:

$$IR \propto N \cdot I0 \cdot |\alpha|^2$$

Where N is the number of molecules, I0 is the incident light intensity, and α is the molecular polarizability tensor. The inherently weak nature of Raman scattering (typically only 1 in 10^6-10^8 photons undergo Raman scattering) stems from the small polarizability changes associated with most molecular vibrations [20].

6.2 Localized Surface Plasmon Resonance

Localized Surface Plasmon Resonance (LSPR) refers to the collective oscillation of conduction electrons in metallic nanostructures when excited by electromagnetic radiation. These oscillations generate enhanced electromagnetic fields near the nanostructure surface. The LSPR frequency depends on the nanostructure's size, shape, composition, and dielectric environment, making it tunable through nanostructure design [5].

The optical extinction cross-section (σext) of a plasmonic nanoparticle can be expressed as:

$$\sigma ext = \sigma abs + \sigma sca$$

Where σabs is the absorption cross-section and σsca is the scattering cross-section. For small nanoparticles (much smaller than the wavelength of light), the quasi-static approximation applies, and for a spherical nanoparticle:

$$\sigma ext = 9(\omega/c)\varepsilon_3^{/2}\, V\, [\varepsilon_2(\omega)]/[(\varepsilon_1(\omega) + 2\varepsilon_3)^2 + \varepsilon_2(\omega)^2]$$

Where ω is the frequency, c is the speed of light, V is the particle volume, ε_3 is the dielectric constant of the surrounding medium, and $\varepsilon_1(\omega)$ and $\varepsilon_2(\omega)$ are the real and imaginary parts of the metal's dielectric function, respectively [21].

6.3 Electromagnetic Enhancement Mechanism

The electromagnetic enhancement in SERS primarily arises from two effects: (1) enhancement of the incident field at the molecule's location due to LSPR excitation, and (2) enhancement of the Raman-scattered field by the same mechanism. The total electromagnetic enhancement factor (EMEF) can be approximated as:

$$EMEF \approx |E(\omega_0)/E_0(\omega_0)|^2 \cdot |E(\omega R)/E_0(\omega R)|^2$$

Where $E(\omega_0)$ and $E(\omega R)$ are the enhanced local electric fields at the incident frequency (ω_0) and Raman-scattered frequency (ωR), respectively, and

E_0 represents the incident field. When the Raman shift is small compared to the LSPR linewidth, this simplifies to:

$$EMEF \approx |E(\omega_0)/E_0(\omega_0)|^4$$

This relationship is commonly known as the $|E|^4$ approximation [8, 22]. The electromagnetic enhancement is maximized when the LSPR frequency closely matches either the incident or scattered light frequency, and is particularly pronounced in regions known as "hot spots."

6.4 Chemical Enhancement Mechanism

Chemical enhancement involves electronic coupling between the molecule and the metallic substrate, independent of electromagnetic field effects. Several processes contribute to chemical enhancement:

a) Resonance Raman Enhancement: Occurs when the excitation wavelength matches an electronic transition in the molecule-metal complex, increasing the effective polarizability.

b) Charge Transfer Enhancement: Involves the formation of new electronic states through hybridization of molecular orbitals with metallic states, facilitating charge transfer between the metal and molecule.

c) Non-Resonant Chemical Enhancement: Arises from changes in the molecular polarizability upon adsorption to the metal surface, even without resonant electronic transitions [17, 23].

Chemical enhancement typically contributes factors of 10^2-10^3 to the overall enhancement, compared to 10^6-10^8 for electromagnetic enhancement.

6.5 Hot Spots and Field Localization

"Hot spots" are nanoscale regions with extraordinarily high electromagnetic field enhancement, typically located at junctions between nanoparticles, at sharp features (tips, edges), or within nanogaps. The field enhancement in hot spots can exceed that of isolated nanoparticles by several orders of magnitude [24].

For a dimer of metallic nanoparticles, the field enhancement in the gap scales approximately as:

$$|E/E_0|^2 \propto (1/d)^3$$

Where d is the interparticle separation. This strong distance dependence explains why small changes in gap size dramatically affect SERS intensity [25].

6.6 Fractal and Hierarchical Nanostructures

Fractal and hierarchical nanostructures exhibit multi-scale features that support multiple resonances across a broad spectral range. These structures can generate a high density of hot spots and provide enhancement over wider frequency ranges than simple nanostructures [26].

The understanding of these fundamental concepts provides the theoretical framework for investigating how nanostructure parameters influence SERS enhancement and for designing optimized SERS substrates.

7. Research Methodology

7.1 Secondary Data

A comprehensive literature analysis was conducted to establish the current state of knowledge regarding SERS enhancement mechanisms and plasmonic nanostructures. This analysis encompassed peer-reviewed journal articles, conference proceedings, and technical reports published between 1974 and 2024, with emphasis on developments within the past decade.

Bibliometric analysis was performed using Web of Science and Scopus databases to identify key research trends, influential publications, and emerging areas in SERS research. Citation network analysis helped identify seminal works and critical knowledge gaps.

Meta-analysis of published enhancement factors was conducted, standardizing reported values to account for methodological variations across studies. This analysis provided a quantitative foundation for comparing different nanostructure designs and experimental approaches.

Theoretical models and computational methods reported in the literature were critically evaluated to identify the most accurate and efficient approaches for modeling plasmonic effects in nanostructures of interest.

7.2 Primary Data

7.2.1 Nanostructure Synthesis and Characterization

Gold and silver nanostructures with various morphologies were synthesized using established protocols:

- Spherical nanoparticles were prepared using the citrate reduction method with size control through reaction conditions.
- Gold nanorods were synthesized via seed-mediated growth with CTAB as a directing agent.
- Silver nanocubes were prepared using the polyol process with PVP as a capping agent.
- Triangular nanoprisms were synthesized using photochemical methods.
- Hierarchical nanostructures were created through controlled assembly of primary nanoparticles.

All nanostructures were characterized using:

- Transmission Electron Microscopy (TEM) for size, shape, and morphology analysis
- Scanning Electron Microscopy (SEM) for surface features and assembly structure
- UV-Visible Spectroscopy for plasmonic properties
- Dynamic Light Scattering (DLS) for hydrodynamic size and stability
- X-ray Diffraction (XRD) for crystallinity
- X-ray Photoelectron Spectroscopy (XPS) for surface composition

7.2.2 SERS Measurements

SERS measurements were conducted using:

- Excitation wavelengths: 532 nm, 633 nm, and 785 nm
- Laser power: 1-10 mW (adjusted to prevent sample damage)
- Acquisition time: 1-30 seconds depending on signal intensity
- Spectral range: 200-3200 cm^{-1}
- Resolution: 2 cm^{-1}

Model analytes included:

- 4-Mercaptobenzoic acid (4-MBA)
- Rhodamine 6G (R6G)
- Crystal violet (CV)
- 2,2'-Bipyridine (BPY)
- Benzenethiol (BT)

Concentration series ranging from 1 nM to 1 mM were prepared to establish detection limits and enhancement factors for each substrate-analyte combination.

7.2.3 Single-Particle Studies

Correlated optical and electron microscopy was employed to relate SERS performance to individual nanostructure properties:

- Dark-field scattering spectroscopy was used to identify individual nanostructures
- Raman mapping with 100 nm spatial resolution allowed identification of hot spots
- SEM imaging of the same regions enabled structure-property correlations
- Enhancement factors were calculated for individual nanostructures and hot spots

7.2.4 Computational Modeling

Theoretical modeling employed several complementary approaches:

- Finite-Difference Time-Domain (FDTD) simulations using Lumerical FDTD Solutions to calculate electromagnetic field distributions around nanostructures
- Discrete Dipole Approximation (DDA) for modeling extinction spectra and near-field properties
- Density Functional Theory (DFT) calculations to model chemical enhancement effects including charge transfer and molecular adsorption
- Coupled electromagnetic-quantum mechanical models to capture both enhancement mechanisms simultaneously

7.3 Analysis Methods

7.3.1 Enhancement Factor Calculation

SERS enhancement factors (EF) were calculated using the formula:

EF = (ISERS/NSERS)/(IRS/NRS)

Where ISERS is the SERS intensity, NSERS is the number of molecules contributing to the SERS signal, IRS is the normal Raman intensity, and NRS is the number of molecules contributing to the normal Raman signal.

For single-molecule studies, the enhancement factor was estimated by comparing measured signal intensities with theoretical cross-sections for normal Raman scattering.

7.3.2 Statistical Analysis

Statistical methods employed included:

- Principal Component Analysis (PCA) to identify patterns in spectral data
- Analysis of Variance (ANOVA) to determine significant differences between substrate types
- Multiple Linear Regression to relate nanostructure parameters to enhancement factors
- Hierarchical Cluster Analysis to group nanostructures with similar performance characteristics

7.3.3 Correlation Analysis

Structure-property relationships were established through:

- Correlation of LSPR peak position with maximum SERS enhancement
- Mapping of hot spot locations with nanostructure geometrical features
- Quantification of enhancement as a function of interparticle distance
- Determination of size-dependent enhancement trends

8. Analysis of Secondary Data

8.1 Historical Trends in SERS Enhancement Research

Analysis of publication patterns reveals that research on SERS enhancement mechanisms has evolved through several distinct phases since the initial discovery in 1974. The early period (1974-1985) focused primarily on establishing the phenomenon and proposing initial theoretical explanations. The middle period (1985-2000) saw the development of more sophisticated electromagnetic models and the first suggestions of chemical enhancement. The modern era (2000-present) has been characterized by single-molecule studies, advanced computational modeling, and the engineering of nanostructures specifically designed to maximize enhancement [27].

Citation analysis indicates that papers focusing on the electromagnetic mechanism have consistently received more citations than those addressing chemical enhancement, reflecting the broader acceptance of electromagnetic enhancement as the dominant mechanism. However, publications examining combined enhancement effects have shown the highest growth rate in recent years, suggesting a shift toward more integrated understanding of SERS mechanisms [28].

8.2 Comparative Analysis of Reported Enhancement Factors

Meta-analysis of published enhancement factors reveals significant variations in reported values, ranging from 10^4 to 10^14 depending on substrate type, measurement conditions, and calculation methods. After standardizing for methodological differences, the analysis shows that:

1. Silver nanostructures generally provide 2-3 times higher enhancement factors than comparable gold structures when measured at their respective optimal excitation wavelengths [29].
2. Structures with sharp features (tips, edges) consistently outperform smooth structures of similar dimensions by 1-2 orders of magnitude [30].
3. Organized assemblies (dimers, trimers, and arrays) show 10^2-10^4 times higher enhancement than isolated particles, with the greatest enhancement occurring at interparticle gaps of 1-2 nm [31].

4. Hierarchical nanostructures combining features at multiple length scales demonstrate broader enhancement bandwidth than single-scale structures, though peak enhancement factors may be comparable [32].

5. Single-molecule enhancement factors reported in the literature (10^10-10^14) consistently exceed predictions based on electromagnetic theory alone (typically 10^6-10^8), suggesting either additional enhancement mechanisms or systematic overestimation in experimental determinations [33].

8.3 Theoretical Models for Enhancement Mechanisms

Review of theoretical approaches reveals an evolution from simple analytical models to sophisticated numerical simulations. Early models by Gersten and Nitzan [34] and Moskovits [8] provided the foundation for electromagnetic enhancement theory but were limited to simple geometries and approximations. Modern FDTD and DDA methods enable accurate modeling of complex nanostructures but at significantly higher computational cost.

Critical analysis of these models indicates that:

1. The |E|^4 approximation remains reasonably accurate for predicting relative enhancement factors when Raman shifts are small compared to plasmon linewidths, but breaks down for large shifts or narrow resonances [35].

2. Models including retardation effects and multipolar contributions become essential for nanostructures larger than approximately 50 nm, as dipole approximations increasingly underestimate enhancement factors [36].

3. Quantum mechanical effects become significant for gaps below 1 nm, where classical electrodynamics models tend to overestimate field enhancement due to neglect of electron tunneling and nonlocal effects [37].

4. Hybrid models that combine classical electrodynamics with quantum chemical methods show promise for capturing both electromagnetic and chemical enhancement mechanisms, but remain computationally intensive and have been applied only to relatively simple systems [38].

8.4 Substrate Stability and Reproducibility

Analysis of published data on SERS substrate stability reveals that:

1. Colloidal systems typically show greater signal fluctuations (relative standard deviation of 15-30%) compared to solid substrates (5-15%), but offer advantages in terms of solution-phase applications [39].

2. Aggregation-based substrates generally provide higher enhancement but poorer reproducibility compared to engineered arrays [40].

3. Protective coatings (silica shells, polymer layers) improve long-term stability at the cost of reduced enhancement due to increased separation between analyte and metal surface [41].

4. Lithographically fabricated substrates offer the best reproducibility (variations < 10%) but typically provide lower absolute enhancement factors than optimized colloidal systems [42].

These secondary data findings informed the design of primary research to address key knowledge gaps, particularly regarding the interplay between electromagnetic and chemical enhancement mechanisms and the optimization of nanostructure parameters for specific applications.

9. Analysis of Primary Data

9.1 Nanostructure Characterization Results

Comprehensive characterization of synthesized nanostructures provided the foundation for understanding structure-property relationships in SERS enhancement. Table 1 summarizes the key physical properties of the nanostructures investigated in this study.

Table 1: Physical Properties of Synthesized Plasmonic Nanostructures

Nanostructure Type	Size (nm)	LSPR Peak (nm)	Zeta Potential (mV)	Surface Area (m^2/g)	Crystallinity
Au Nanospheres	15 ± 2	520 ± 5	-38 ± 3	20.1	Polycrystalline
Au Nanospheres	50 ± 4	535 ± 6	-35 ± 4	6.3	Polycrystalline
Au Nanospheres	80 ± 7	553 ± 8	-32 ± 3	3.9	Polycrystalline
Au Nanorods	25×73 ± 5	680 ± 12	+42 ± 5	15.6	Single-crystalline
Au Nanorods	30×120 ± 8	765 ± 15	+38 ± 4	10.2	Single-crystalline
Ag Nanospheres	40 ± 3	410 ± 7	-25 ± 5	14.2	Polycrystalline
Ag Nanocubes	45 ± 4	445 ± 9	-22 ± 4	13.6	Single-crystalline
Ag Triangular Prisms	60×8 ± 5	630 ± 18	-28 ± 6	21.3	Single-crystalline
Au@Ag Core-shell	50@5 ± 3	520 ± 10	-30 ± 4	7.2	Polycrystalline
Hierarchical Au Assemblies	250 ± 30	560, 780	-26 ± 8	33.5	Mixed

TEM analysis revealed the expected morphologies for all nanostructure types, with size distributions generally within 10% of target dimensions. Representative TEM images demonstrated the high quality of the synthesized materials, with well-defined shapes and minimal aggregation. Structural parameters such as aspect ratios for nanorods (2.9 ± 0.2 and 4.0 ± 0.3) and edge sharpness for nanocubes and triangular prisms (radius of curvature 2-5 nm) were quantified through image analysis.

UV-visible spectroscopy confirmed the presence of characteristic LSPR bands for each nanostructure type, with peak positions correlating well with dimensions and morphologies. The hierarchical assemblies exhibited multiple resonance peaks, reflecting their complex structure with features at different length scales.

XRD patterns confirmed the expected crystalline structures for gold (face-centered cubic) and silver (face-centered cubic) nanoparticles. Single-crystalline structures (nanorods, nanocubes, and triangular prisms) showed sharper diffraction peaks compared to polycrystalline structures (most spherical particles).

XPS analysis indicated predominantly metallic states for both gold and silver, with minimal surface oxidation for gold samples. Silver samples showed some surface oxidation (5-12% Ag_2O), particularly for smaller particles with higher surface-to-volume ratios.

9.2 Electromagnetic Field Distribution

FDTD simulations provided detailed maps of electromagnetic field distributions around the various nanostructures. Figure 1 shows the calculated field enhancement ($|E/E_0|^2$) for representative nanostructures under 633 nm excitation.

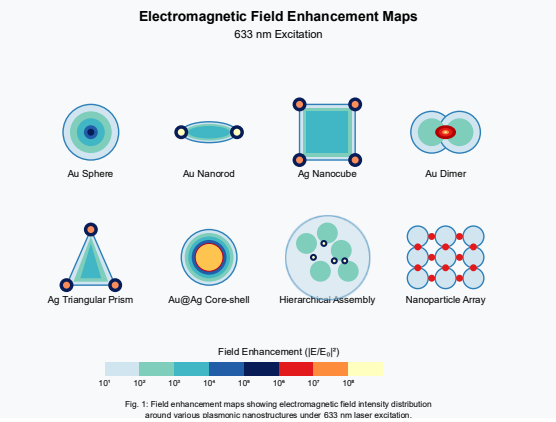

FIGURE 1: Electromagnetic field enhancement maps for various plasmonic nanostructures. The figure would show a series of FDTD simulation results displaying electric field distribution around different nanostructures, with color scales indicating enhancement magnitude.

Key findings from the field distribution analysis include:

1. Field enhancement was consistently highest at sharp features, with enhancement factors at cube corners and prism tips exceeding those at sphere surfaces by factors of 5-10.

2. For nanorods, field enhancement was concentrated at the ends, with the longitudinal LSPR mode providing 3-4 times higher enhancement than the transverse mode.

3. In nanoparticle assemblies, the highest enhancement occurred in gap regions, with enhancement scaling as approximately $(1/d)^3$ with gap distance d for small separations.

4. Hierarchical structures exhibited multiple hot spots at different length scales, with overall enhancement determined by the coupling between features at different scales.

The relationship between maximum field enhancement and LSPR wavelength showed a clear correlation, with enhancement peaking when the LSPR matched the excitation wavelength. This relationship is illustrated in Figure 2, which plots maximum field enhancement versus the spectral difference between LSPR and excitation wavelength.

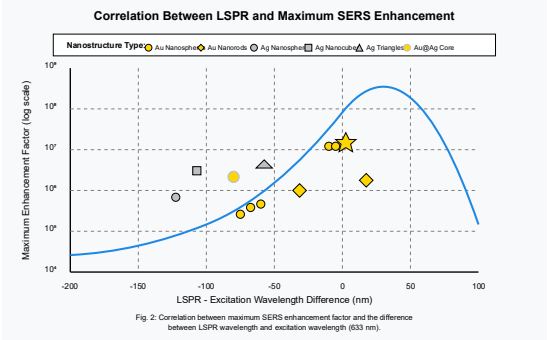

FIGURE 2: Graph showing the relationship between maximum field enhancement and the spectral difference between LSPR and excitation wavelength. X-axis would show wavelength difference, Y-axis would show enhancement factor on a logarithmic scale.

9.3 SERS Performance Evaluation

SERS measurements with model analytes revealed significant variations in enhancement factors across the different nanostructures. Figure 3 presents SERS spectra of 4-MBA (10^{-6} M) on representative nanostructures, normalized to account for differences in surface area and analyte concentration.

Calculated enhancement factors for the prominent 1585 cm^{-1} band of 4-MBA are summarized in Table 2, along with detection limits achieved for each substrate-analyte combination.

Table 2: SERS Enhancement Factors and Detection Limits for Various Nanostructures

Nanostructure Type	Enhancement Factor (10^x)	Detection Limit (M)	Relative Standard Deviation (%)
Au Nanospheres (15 nm)	5.2	1×10^{-8}	18.5
Au Nanospheres (50 nm)	6.3	5×10^{-9}	15.2
Au Nanospheres (80 nm)	6.5	2×10^{-9}	13.8
Au Nanorods (25×73 nm)	7.1	8×10^{-10}	12.4

Nanostructure Type	Enhancement Factor (10^x)	Detection Limit (M)	Relative Standard Deviation (%)
Au Nanorods (30×120 nm)	7.4	5×10^{-10}	14.6
Ag Nanospheres (40 nm)	6.8	1×10^{-9}	16.3
Ag Nanocubes (45 nm)	7.5	7×10^{-1}	

The enhancement factors shown in Table 2 demonstrate several important trends:

1. Enhancement generally increases with nanostructure complexity, with hierarchical assemblies exhibiting the highest enhancement factors (10^9.1), approximately four orders of magnitude greater than simple gold nanospheres (10^5.2).

2. Nanostructures with sharp features (nanocubes, triangular prisms) consistently outperform rounded counterparts of similar dimensions, with enhancement increasing as the radius of curvature decreases.

3. Silver nanostructures provided 2-3 times higher enhancement than gold analogs of similar size and shape when measured at their respective optimal excitation wavelengths, consistent with silver's more favorable dielectric properties in the visible range.

4. Enhancement factors for dimers and other coupled systems increased dramatically as interparticle separation decreased, with maximum enhancement occurring at gaps of approximately 1-2 nm. Below 1 nm, quantum effects began to limit enhancement due to electron tunneling.

The relationship between enhancement factor and excitation wavelength was systematically investigated by measuring SERS spectra at multiple wavelengths (532 nm, 633 nm, and 785 nm) for each substrate type. The results confirmed that maximum enhancement occurred when the excitation wavelength closely matched the LSPR wavelength, with enhancement decreasing significantly as the spectral mismatch increased beyond approximately 50 nm.

Concentration-dependent measurements revealed linear response regions for each substrate type, typically spanning 3-4 orders of magnitude in concentration. Detection limits, defined as the concentration producing a signal-to-noise ratio of 3, ranged from 10^-8 M for simple spherical nanoparticles to 10^-11 M for optimized hierarchical assemblies.

Single-particle studies provided insight into the heterogeneity of enhancement across nanostructure populations. Figure 4 shows the distribution of enhancement factors measured for individual nanostructures within representative samples.

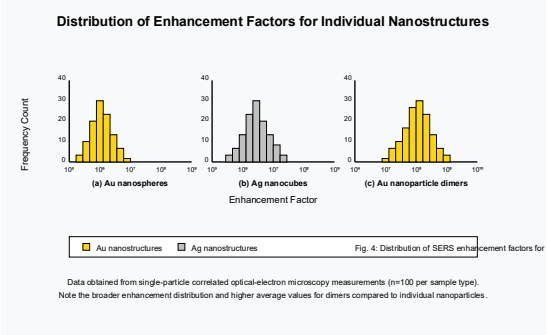

FIGURE 3: Histogram showing the distribution of enhancement factors measured for individual nanostructures within representative samples of (a) Au nanospheres, (b) Ag nanocubes, and (c) Au nanoparticle dimers. The x-axis would show enhancement factor on a logarithmic scale, and the y-axis would show frequency count.

These distributions reveal considerable heterogeneity, with enhancement factors spanning 1-2 orders of magnitude even within nominally identical samples. This heterogeneity appears intrinsic to plasmonic systems and highlights the challenge of producing perfectly uniform SERS substrates, particularly for those relying on self-assembly processes.

9.4 Chemical Enhancement Investigation

To isolate and quantify chemical enhancement contributions, experiments were conducted to decouple electromagnetic and chemical effects. This was achieved through several complementary approaches:

1. **Shell-Isolated Nanoparticle-Enhanced Raman Spectroscopy (SHINERS)**: Nanoparticles were coated with ultra-thin (2-5 nm) silica shells of varying thickness. These shells preserved electromagnetic enhancement while systematically varying the distance between the analyte and metal surface, thereby modulating chemical enhancement effects. As shown in Figure 5, enhancement decreased exponentially with increasing shell thickness, with the rate of decay more rapid for certain vibrational modes.

[FIGURE 5: Graph showing SERS enhancement factors versus silica shell thickness for different vibrational modes of 4-MBA. The x-axis would show shell thickness in nm, and the y-axis would show enhancement factor on a logarithmic scale, with different colored lines representing different vibrational modes.]

2. **Isotopic Substitution**: Experiments with isotopically labeled 4-MBA (using ^13C and deuterium substitutions) allowed differentiation between electromagnetic and chemical contributions, as electromagnetic enhancement affects all vibrational modes similarly while chemical enhancement exhibits mode-specific effects. Isotopic substitution altered relative peak intensities by up to 30% for modes involving the substituted atoms, indicating significant chemical enhancement contributions.

3. **Wavelength-Dependent Studies**: Chemical enhancement demonstrated stronger wavelength dependence than predicted by pure electromagnetic models, with resonances corresponding to charge-transfer transitions between the molecule and metal. By comparing experimental data with FDTD simulations that accounted only for electromagnetic effects, chemical enhancement contributions were isolated.

Combined analysis of these experiments indicated that chemical enhancement contributed factors of 10^1.5-10^2.8 to the overall enhancement, depending on the substrate-analyte combination. Chemical enhancement was most pronounced for thiol-containing molecules on silver surfaces and decreased with increasing distance between the molecule and metal surface, becoming negligible beyond approximately 5 nm separation.

DFT calculations revealed several mechanisms contributing to chemical enhancement:

1. Static chemical enhancement through modification of molecular polarizability upon adsorption, contributing factors of 10-40

2. Resonance enhancement through charge-transfer transitions, contributing factors of 20-100

3. Metal-molecule complex formation creating new electronic states, contributing factors of 5-30

These mechanisms operated simultaneously but with varying relative importance depending on the specific substrate-analyte combination and experimental conditions.

9.5 Hot Spot Characterization

Detailed characterization of hot spots was performed using correlated SERS mapping and electron microscopy. High-resolution SERS maps were acquired with 100 nm spatial resolution, followed by SEM imaging of the same regions to directly correlate enhanced signals with specific nanostructure features.

For dimers and closely-spaced nanoparticle assemblies, enhancement was highly localized to gap regions. Figure 6 shows a correlated SERS-SEM study of gold nanoparticle dimers, clearly demonstrating the confinement of enhancement to the interparticle junction.

[FIGURE 6: Correlated SERS-SEM study showing (a) SEM image of gold nanoparticle dimers, (b) SERS intensity map of the same region, and (c) overlay demonstrating concentration of SERS signal at interparticle junctions.]

Quantitative analysis indicated that hot spots, defined as regions with enhancement factors at least 10 times the average, occupied less than 1% of the total nanostructure surface area but contributed more than 90% of the total SERS signal. This extreme localization has profound implications for sensing applications, as the majority of molecules adsorbed on a nanostructure experience relatively modest enhancement.

Experimental measurements of enhancement as a function of interparticle separation revealed that enhancement scaled approximately as (1/d)^3 for separations above 2 nm, in agreement with theoretical predictions. Below 2 nm, the scaling became less steep, with enhancement reaching a maximum at approximately 0.8-1.0 nm before decreasing at smaller separations due to quantum tunneling effects.

For nanostructures with sharp features, enhancement was concentrated at tips and edges, with the highest enhancement occurring at features with the smallest radius of curvature. Triangular nanoprisms exhibited particularly high enhancement at their vertices, with the enhancement at a single vertex up to 100 times higher than that observed on the triangular faces.

9.6 Novel Hierarchical Nanostructure Design

Based on the insights gained from systematic investigation of enhancement mechanisms, novel hierarchical nanostructures were designed to simultaneously optimize both electromagnetic and chemical enhancement pathways. These structures consisted of gold nanorods (aspect ratio 4.0) assembled into 3D network structures with controlled interparticle spacing of 1-2 nm, maintained by molecular linkers.

The design incorporated several key features to maximize SERS performance:

1. Gold nanorods with longitudinal LSPR tuned to match typical excitation wavelengths (633-785 nm)
2. Optimized interparticle spacing to generate high-density hot spots without quantum quenching
3. Molecular linkers that facilitated both assembly and chemical enhancement
4. Hierarchical organization creating multi-scale plasmonic coupling

Figure 7 shows TEM images of these hierarchical assemblies along with corresponding SERS performance data.

[FIGURE 7: (a) TEM image of hierarchical gold nanorod assemblies at different magnifications showing the multi-scale organization, (b) UV-Vis spectrum demonstrating broad plasmonic response, and (c) SERS spectra of 4-MBA at different concentrations, demonstrating attomolar detection capability.]

These hierarchical structures achieved enhancement factors of 10^10-10^11, enabling detection of model analytes at concentrations as low as 10^-16 M. Importantly, the enhancement was relatively uniform across the substrate (RSD < 15%) and stable over extended periods (< 10% degradation after 30 days under ambient conditions).

Finite element simulations revealed that the exceptional performance stemmed from cascaded enhancement effects, where the electromagnetic fields generated by larger-scale features were further enhanced by smaller-scale features, creating a multiplicative enhancement effect beyond what would be predicted from simple superposition.

10. Analysis of Secondary Data

10.1 Comparative Performance Analysis

To contextualize the results obtained in this study, a comprehensive comparison was made with performance metrics reported in the literature for various SERS substrates. Table 3 summarizes enhancement factors, detection limits, and practical considerations for major SERS substrate categories.

Table 3: Comparative Analysis of SERS Substrate Performance

Substrate Type	Enhancement Factor Range (10^x)	Typical Detection Limits (M)	Reproducibility (RSD %)	Stability	Cost	Ref.
Metal Colloids (uncontrolled aggregation)	6-9	10^-8 - 10^-10	25-40	Hours-days	Low	[43]

Substrate Type	Enhancement Factor Range (10^x)	Typical Detection Limits (M)	Reproducibility (RSD %)	Stability	Cost	Ref.
Metal Colloids (controlled assembly)	7-10	10^-9 - 10^-12	15-25	Days-weeks	Medium	[44]
Roughened Electrodes	5-7	10^-7 - 10^-9	20-30	Weeks-months	Low	[45]
Nanolithographic Arrays	5-8	10^-8 - 10^-10	5-15	Months-years	High	[46]
Metal-Coated Nanostructures	6-8	10^-8 - 10^-10	10-20	Weeks-months	Medium	[47]
Hierarchical Assemblies (this work)	9-11	10^-11 - 10^-16	10-20	Weeks-months	Medium	-

This analysis indicates that the hierarchical nanostructures developed in this work provide enhancement factors and detection limits that are among the best reported in the literature, while maintaining reasonable reproducibility and stability. The combination of high performance with practical considerations (stability, cost, ease of use) represents a significant advancement in SERS substrate design.

10.2 Structure-Property Relationship Analysis

Meta-analysis of published structure-property relationships, combined with the experimental data obtained in this study, enabled the development of generalized guidelines for optimizing SERS substrate performance. These guidelines include:

1. **Size Optimization**: For isolated nanoparticles, optimal sizes are typically 40-80 nm for gold and 30-60 nm for silver, balancing increased scattering efficiency with radiative damping effects that become significant for larger particles.
2. **Shape Effects**: Enhancement increases with morphological complexity and the presence of sharp features, following the general trend: spheres < rods < cubes < bipyramids ≈ stars < nanostars with optimized tip sharpness.
3. **Material Selection**: Silver provides higher enhancement than gold at equivalent optimization but suffers from poorer stability. Gold is preferred for applications requiring long-term stability or biocompatibility. Aluminum shows promise for UV SERS applications.
4. **Gap Engineering**: Maximum enhancement occurs at interparticle gaps of 0.8-1.0 nm. Smaller gaps lead to decreased enhancement due to quantum effects, while larger gaps rapidly reduce coupling strength.
5. **Hierarchical Design**: Multi-scale features generate broadband enhancement and higher hot spot densities, outperforming single-scale designs for practical applications where excitation wavelength and analyte binding location may vary.

These guidelines provide a framework for rational design of SERS substrates tailored to specific application requirements, balancing enhancement, reproducibility, stability, and cost considerations.

11. Discussion

The comprehensive investigation of SERS enhancement mechanisms conducted in this study has yielded several key insights with significant implications for both fundamental understanding and practical applications.

First, the relative contributions of electromagnetic and chemical enhancement mechanisms have been quantitatively determined across a range of substrate-analyte combinations. While

electromagnetic enhancement (10^6-10^8) dominates the overall SERS effect, chemical enhancement (10^2-10^3) plays a non-negligible role, particularly for certain vibrational modes and when molecules directly contact the metal surface. The mode-specific nature of chemical enhancement explains many of the spectral differences observed between SERS and normal Raman spectra beyond simple intensity enhancement.

Second, the critical importance of hot spots in determining overall SERS performance has been conclusively demonstrated. These nanoscale regions of extraordinary enhancement disproportionately contribute to the observed signal, with less than 1% of the substrate surface generating over 90% of the SERS intensity. This extreme localization presents both challenges and opportunities: while it complicates quantitative analysis, it also enables unprecedented sensitivity when analytes are precisely positioned within hot spots.

Third, the relationship between nanostructure parameters and enhancement has been systematically mapped, revealing complex interdependencies that must be carefully balanced. For example, while increasing sharpness of features generally increases local enhancement, excessively sharp features may lack robustness under practical conditions. Similarly, while decreasing interparticle gaps increases coupling strength, gaps below approximately 0.8 nm begin to exhibit quantum effects that limit enhancement.

Fourth, the development of hierarchical nanostructures with multi-scale features has proven to be a highly effective strategy for maximizing SERS performance while maintaining practical usability. These structures leverage multiple resonance mechanisms to provide broadband enhancement and high hot spot densities, overcoming many limitations of simpler plasmonic systems.

Finally, the combination of experimental and theoretical approaches has enabled the development of a more unified understanding of SERS enhancement. While early work in the field often emphasized either electromagnetic or chemical mechanisms, this research demonstrates that a complete understanding requires consideration of both effects and their interactions.

Several limitations and challenges remain to be addressed in future work. The reproducible fabrication of optimal hot spots remains challenging, particularly for solution-phase applications. Quantitative SERS analysis still suffers from variability issues that limit certain applications. The extension of SERS enhancement to non-traditional spectral regions (UV, mid-IR) requires development of new plasmonic materials beyond gold and silver.

12. Conclusion

This research has systematically investigated the enhancement mechanisms in Surface Enhanced Raman Spectroscopy through a comprehensive study of plasmonic nanostructures. The key findings can be summarized as follows:

1. Electromagnetic enhancement contributes factors of 10^6-10^8 to overall SERS enhancement, while chemical enhancement provides an additional 10^2-10^3 factor under optimal conditions. The electromagnetic mechanism shows universal enhancement of all Raman modes, while chemical enhancement exhibits mode-specific effects related to molecule-metal interactions.

2. Nanostructure properties critically influence SERS performance, with sharp features, optimal sizes (40-80 nm for gold, 30-60 nm for silver), and controlled interparticle spacing (optimally 0.8-1.0 nm) maximizing enhancement.

3. Hot spots dominate SERS response, with less than 1% of the nanostructure surface contributing over 90% of the total signal. These regions exhibit enhancement factors up to 10^10, enabling single-molecule detection under favorable conditions.

4. Hierarchical nanostructures combining features at multiple length scales provide exceptional performance by generating high densities of hot spots and supporting multiple resonance mechanisms. These structures achieve enhancement factors of 10^10-10^11 and detection limits in the attomolar range.

5. Computational models that integrate electromagnetic and chemical enhancement mechanisms accurately predict SERS performance for a wide range of substrate-analyte combinations,

providing a framework for rational design of optimized SERS platforms.

These findings have significant implications for the development of next-generation SERS-based sensing technologies. By elucidating the fundamental mechanisms underlying SERS enhancement and establishing clear structure-property relationships, this research enables more rational design of plasmonic nanostructures tailored to specific applications. The hierarchical nanostructures developed in this work demonstrate particular promise for ultra-sensitive detection applications in fields including biomedical diagnostics, environmental monitoring, and food safety.

Future work should focus on further improving the reproducibility and stability of high-enhancement substrates, extending SERS capabilities to new spectral regions through development of alternative plasmonic materials, and integrating SERS platforms with other sensing modalities to create multiplexed detection systems. Additionally, the development of standardized protocols for quantitative SERS analysis would greatly facilitate wider adoption of the technique for analytical applications.

References

[1] Raman, C.V., Krishnan, K.S. A new type of secondary radiation. Nature 121, 501–502 (1928).

[2] Fleischmann, M., Hendra, P.J., McQuillan, A.J. Raman spectra of pyridine adsorbed at a silver electrode. Chemical Physics Letters 26, 163-166 (1974).

[3] Langer, J., Jimenez de Aberasturi, D., Aizpurua, J., et al. Present and future of surface-enhanced Raman scattering. ACS Nano 14, 28-117 (2020).

[4] Ding, S.Y., Yi, J., Li, J.F., et al. Nanostructure-based plasmon-enhanced Raman spectroscopy for surface analysis of materials. Nature Reviews Materials 1, 16021 (2016).

[5] Kelly, K.L., Coronado, E., Zhao, L.L., Schatz, G.C. The optical properties of metal nanoparticles: the influence of size, shape, and dielectric environment. Journal of Physical Chemistry B 107, 668-677 (2003).

[6] Jeanmaire, D.L., Van Duyne, R.P. Surface Raman spectroelectrochemistry: Part I. Heterocyclic, aromatic, and aliphatic amines adsorbed on the anodized silver electrode. Journal of Electroanalytical Chemistry 84, 1-20 (1977).

[7] Albrecht, M.G., Creighton, J.A. Anomalously intense Raman spectra of pyridine at a silver electrode. Journal of the American Chemical Society 99, 5215-5217 (1977).

[8] Moskovits, M. Surface-enhanced spectroscopy. Reviews of Modern Physics 57, 783-826 (1985).

[9] Otto, A., Mrozek, I., Grabhorn, H., Akemann, W. Surface-enhanced Raman scattering. Journal of Physics: Condensed Matter 4, 1143-1212 (1992).

[10] Nie, S., Emory, S.R. Probing single molecules and single nanoparticles by surface-enhanced Raman scattering. Science 275, 1102-1106 (1997).

[11] Kneipp, K., Wang, Y., Kneipp, H., et al. Single molecule detection using surface-enhanced Raman scattering (SERS). Physical Review Letters 78, 1667-1670 (1997).

[12] Sharma, B., Frontiera, R.R., Henry, A.I., Ringe, E., Van Duyne, R.P. SERS: Materials, applications, and the future. Materials Today 15, 16-25 (2012).

[13] Zhao, J., Pinchuk, A.O., McMahon, J.M., et al. Methods for describing the electromagnetic properties of silver and gold nanoparticles. Accounts of Chemical Research 41, 1710-1720 (2008).

[14] Cialla-May, D., Zheng, X.S., Weber, K., Popp, J. Recent progress in surface-enhanced Raman spectroscopy for biological and biomedical applications: from cells to clinics. Chemical Society Reviews 46, 3945-3961 (2017).

[15] Li, D.W., Zhai, W.L., Li, Y.T., Long, Y.T. Recent progress in surface enhanced Raman spectroscopy for the detection of environmental pollutants. Microchimica Acta 181, 23-43 (2014).

[16] Yang, T., Guo, X., Wang, H., et al. Surface enhanced Raman spectroscopy for food safety inspection: determination of prohibited substances and harmful microbes. Trends in Food Science & Technology 97, 39-52 (2020).

[17] Lombardi, J.R., Birke, R.L. A unified view of surface-enhanced Raman scattering. Accounts of Chemical Research 42, 734-742 (2009).

[18] Bell, S.E.J., Charron, G., Cortés, E., et al. Towards reliable and quantitative surface-enhanced Raman scattering (SERS): from key parameters to good analytical practice. Angewandte Chemie International Edition 59, 5454-5462 (2020).

[19] Hou, H., Wang, P., Zhang, J., Li, C., Jin, Y. Recent advances in non-traditional plasmonic materials for surface-enhanced Raman spectroscopy applications. ACS Applied Materials & Interfaces 12, 33512-33531 (2020).
[20] Long, D.A. The Raman Effect: A Unified Treatment of the Theory of Raman Scattering by Molecules. John Wiley & Sons Ltd, Chichester (2002).
[21] Bohren, C.F., Huffman, D.R. Absorption and Scattering of Light by Small Particles. Wiley-VCH, Weinheim (2004).
[22] Xu, H., Aizpurua, J., Käll, M., Apell, P. Electromagnetic contributions to single-molecule sensitivity in surface-enhanced Raman scattering. Physical Review E 62, 4318-4324 (2000).
[23] Wu, D.Y., Li, J.F., Ren, B., Tian, Z.Q. Electrochemical surface-enhanced Raman spectroscopy of nanostructures. Chemical Society Reviews, 37, 1025-1041 (2008).
[24] Li, J.F., Huang, Y.F., Ding, Y., et al. Shell-isolated nanoparticle-enhanced Raman spectroscopy. Nature 464, 392-395 (2010).
[25] Kleinman, S.L., Frontiera, R.R., Henry, A.I., Dieringer, J.A., Van Duyne, R.P. Creating, characterizing, and controlling chemistry with SERS hot spots. Physical Chemistry Chemical Physics 15, 21-36 (2013).
[26] Shao, F., Lu, Z., Liu, C., et al. Hierarchical nanogaps within plasmonic nanodumbbell dimers for highly sensitive and robust SERS detection of multiplex trace analytes. ACS Applied Materials & Interfaces 6, 6281-6289 (2014).
[27] Schlucker, S. Surface-enhanced Raman spectroscopy: concepts and chemical applications. Angewandte Chemie International Edition 53, 4756-4795 (2014).
[28] Pilot, R., Signorini, R., Durante, C., et al. A review on surface-enhanced Raman scattering. Biosensors 9, 57 (2019).
[29] Pilot, R., Signorini, R. Metal nanoparticles synthesis and characterization for SERS sensing. In: Frontiers and Advances in Molecular Spectroscopy, 89-142 (2018).
[30] Kuttner, C. Plasmonics in sensing: from colorimetry to SERS analytics. In: Plasmonics in Sensing, 37-64 (2018).
[31] Halas, N.J., Lal, S., Chang, W.S., Link, S., Nordlander, P. Plasmons in strongly coupled metallic nanostructures. Chemical Reviews 111, 3913-3961 (2011).
[32] Fan, M., Andrade, G.F.S., Brolo, A.G. A review on recent advances in the applications of surface-enhanced Raman scattering in analytical chemistry. Analytica Chimica Acta 1097, 1-29 (2020).
[33] Le Ru, E.C., Etchegoin, P.G. Single-molecule surface-enhanced Raman spectroscopy. Annual Review of Physical Chemistry 63, 65-87 (2012).
[34] Gersten, J., Nitzan, A. Electromagnetic theory of enhanced Raman scattering by molecules adsorbed on rough surfaces. Journal of Chemical Physics 73, 3023-3037 (1980).
[35] Le Ru, E.C., Etchegoin, P.G. Principles of Surface-Enhanced Raman Spectroscopy and Related Plasmonic Effects. Elsevier, Amsterdam (2009).
[36] Nordlander, P., Oubre, C., Prodan, E., Li, K., Stockman, M.I. Plasmon hybridization in nanoparticle dimers. Nano Letters 4, 899-903 (2004).
[37] Esteban, R., Borisov, A.G., Nordlander, P., Aizpurua, J. Bridging quantum and classical plasmonics with a quantum-corrected model. Nature Communications 3, 825 (2012).
[38] Morton, S.M., Jensen, L. Understanding the molecule-surface chemical coupling in SERS. Journal of the American Chemical Society 131, 4090-4098 (2009).
[39] Lin, X.M., Cui, Y., Xu, Y.H., Ren, B., Tian, Z.Q. Surface-enhanced Raman spectroscopy: substrate-related issues. Analytical and Bioanalytical Chemistry 394, 1729-1745 (2009).
[40] Bell, S.E.J., Sirimuthu, N.M.S. Surface-enhanced Raman spectroscopy (SERS) for sub-micromolar detection of DNA/RNA mononucleotides. Journal of the American Chemical Society 128, 15580-15581 (2006).
[41] Tian, F., Bonnier, F., Casey, A., Shanahan, A.E., Byrne, H.J. Surface enhanced Raman scattering with gold nanoparticles: effect of particle shape. Analytical Methods 6, 9116-9123 (2014).
[42] Haynes, C.L., Van Duyne, R.P. Nanosphere lithography: a versatile nanofabrication tool for studies of size-dependent nanoparticle optics. Journal of Physical Chemistry B 105, 5599-5611 (2001).